Solar Polarization 6
ASP Conference Series, Vol. 437
Kuhn, Berdyugina, Harrington, Keil, Lin, Rimmele, and Trujillo-Bueno, eds.
© 2011 Astronomical Society of the Pacific

Linear Polarization of the Solar Ca I 4227 Å Line: Modeling with Radiative Transfer and Last Scattering Approximation

L. S. Anusha,[1] J. O. Stenflo,[2,4] H. Frisch,[3] M. Bianda,[4] R. Holzreuter,[2,5] K. N. Nagendra,[1] M. Sampoorna,[1] and R. Ramelli[4]

[1]*Indian Institute of Astrophysics, Koramangala, Bangalore 560 034, India*

[2]*Institute of Astronomy, ETH Zürich, CH-8093 Zürich, Switzerland*

[3]*UNS, CNRS, OCA, Laboratoire Cassiopée, F-06304, Nice Cedex, France*

[4]*Istituto Ricerche Solari Locarno, Via Patocchi, 6605 Locarno-Monti, Switzerland*

[5]*MPI für Sonnensystemforschung, D-37191 Katlenburg-Lindau, Germany*

Abstract. To model the Ca I 4227 Å line polarization, radiative transfer effects with partial frequency redistribution (PRD) must be taken into account. The numerical solution of the relevant polarized radiative transfer (RT) equations is computationally very demanding. The "last scattering approximation" (LSA) is a concept allowing faster methods to be devised. It is based on the remark that a single scattering of the radiation field is sufficient for creating most of the polarization. Its key ingredient is the anisotropy of the radiation field. If the anisotropy is extracted from the observed center to limb variation of the intensity profile, only the wings of the Q/I spectrum can be modeled (Sampoorna et al. 2009). We show here that the core region may be modeled as well if one takes into account the depth variation of the anisotropy which is obtained from an unpolarized multilevel RT code (Anusha et al. 2010). After a validation of the LSA approach by comparison with a polarized RT calculation, we apply both approaches to model recent observations of the Ca I 4227 Å line polarization taken on the quiet Sun. Apart from a global scaling factor, both approaches give a very good fit to the Q/I spectrum for all the wavelengths. As the LSA is 8 times faster than the RT approach, we can recommend it as an efficient method to analyze other strong resonance lines in the second solar spectrum.

1. Introduction

The traditional radiative transfer (RT) approach used for the modeling of the polarized (Q/I) spectra of the Ca I 4226.727 Å line is computationally very demanding. It is well known that this strong resonance line has the highest degree of linear polarization in the visible spectrum. It is formed mainly in the lower chromosphere. The whole polarization profile, including the line wings, is created by resonance scattering. The

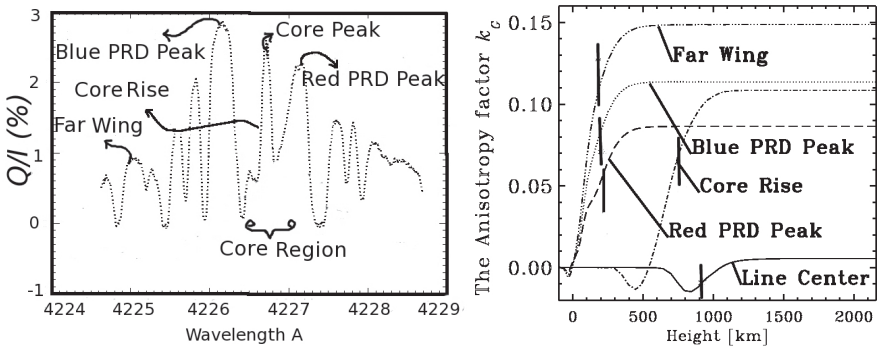

Figure 1. The left panel defines the relevant portions of the observed Q/I profile of the Ca I 4227 Å line. The height dependences of the anisotropy factor k_G at selected wavelengths are shown in the right panel for the FALX model atmosphere. The vertical lines indicate the heights at which $\tau_\lambda/\mu = 1$ for $\mu = 0.11$.

polarization is measurable up to several Doppler widths away from the line center. Because it is a very strong chromospheric resonance line, partial frequency redistribution (PRD) effects have to be accounted for. Faurobert-Scholl (1992, 1994) used the RT approach with the Hanle effect to study the structure of chromospheric magnetic fields. Holzreuter et al. (2005) used the RT approach to interpret the triple-peak structure of the ratio Q/I, common to several chromospheric resonance lines, in terms of PRD and depth variation of the radiation field anisotropy.

Here we describe a new method based on the "last scattering approximation" (LSA) which is much faster than the RT approach and provides a very good modeling of the Q/I profile of this line. A first attempt to use such an approach is described in Sampoorna et al. (2009). With a rather simple form of LSA it was possible to successfully model the Q/I spectrum in the far and near wings. The more elaborate form of LSA described here and in Anusha et al. (2010) can model the whole polarization profile. An alternative approximate method for computing the emergent Q/I profile is that corresponding to Eq. (20) of Sampoorna et al. (2010).

New observations of the Ca I 4227 Å line were made recently. They were taken at IRSOL, Switzerland, using the ZIMPOL-2 polarimeter in the quiet solar regions. The spectrograph slit was placed parallel to the north limb, about 6″ inside, corresponding to an average value of $\mu = 0.11$. The resulting CCD images have effectively 140 pixels in the spatial direction (1.35″/pixel) and 770 pixels in the wavelength direction (5.3 mÅ/pixel). The total integration time per image was 10 minutes. For further details on the observations, see Bianda et al. (2010) in this proceedings. The left panel of Figure 1 shows a high resolution observation of the Q/I profile for the wavelength region ±2 Å about the line center. One can observe the well known triple-peak structure, namely a central core peak surrounded by asymmetric wing peaks. These peaks are known to be caused by the PRD scattering mechanisms. In the far wings the level of the continuum polarization is approached.

We first describe the traditional RT approach and then our LSA approach. The LSA approach is validated by comparisons with RT benchmarks. We then show how it may be used in the modeling of the linear polarization profile of the Ca I 4227 Å line.

2. The Radiative Transfer Approach

The polarized RT equation in a one-dimensional planar axisymmetric medium can be written as

$$\mu \frac{\partial \boldsymbol{I}(\lambda, \mu, z)}{\partial z} = -\kappa_{tot}(\lambda, z) \left[\boldsymbol{I}(\lambda, \mu, z) - \boldsymbol{S}(\lambda, \mu, z) \right], \tag{1}$$

where $\boldsymbol{I} = (I, Q)^T$ is the Stokes vector. We follow the same standard notation as in Anusha et al. (2010). In a 2-level atom model, the total source vector $\boldsymbol{S} = (S_I, S_Q)^T$ is

$$\boldsymbol{S}(\lambda, \mu, z) = \frac{\kappa_l(z)\phi(\lambda, z)\boldsymbol{S}_l(\lambda, \mu, z) + \sigma_c(\lambda, z)\boldsymbol{S}_c(\lambda, \mu, z) + \kappa_c(\lambda, z)\boldsymbol{B}(\lambda, z)}{\kappa_{tot}(\lambda, z)}, \tag{2}$$

with

$$\kappa_{tot}(\lambda, z) = \kappa_l(z)\phi(\lambda, z) + \sigma_c(\lambda, z) + \kappa_c(\lambda, z). \tag{3}$$

The line source vector $\boldsymbol{S}_l = (S_{I,l}, \ S_{Q,l})^T$ is given by

$$\boldsymbol{S}_l(\lambda, \mu, z) = \frac{(1-\epsilon)}{\phi(\lambda, z)} \int_{-1}^{+1} \frac{\mathrm{d}\mu'}{2} \int_0^{\infty} \mathrm{d}\lambda' \hat{\boldsymbol{R}}(\lambda, \lambda', \mu, \mu', z) \, \boldsymbol{I}(\lambda', \mu', z) + \epsilon \boldsymbol{B}(\lambda, z). \tag{4}$$

$\epsilon = \Gamma_I/(\Gamma_R + \Gamma_I)$ is the thermalization parameter. The partial frequency redistribution (PRD) matrix $\hat{\boldsymbol{R}}(\lambda, \lambda', \mu, \mu', z)$ contains the physics of the scattering mechanism (see e.g., Domke & Hubeny 1988; Bommier 1997). The formal solution of Equation (1) can be written as

$$\boldsymbol{I}(\lambda, \mu, \tau_\lambda) = \boldsymbol{I}_0(\lambda, \mu, T_\lambda) \exp\left[-\left(\frac{T_\lambda - \tau_\lambda}{\mu} \right) \right] + \int_{\tau_\lambda}^{T_\lambda} \exp\left[-\left(\frac{\tau'_\lambda - \tau_\lambda}{\mu} \right) \right] \boldsymbol{S}(\lambda, \mu, \tau'_\lambda) \frac{\mathrm{d}\tau'_\lambda}{\mu}, \tag{5}$$

for $\mu > 0$ (the outgoing rays). A similar expression holds for $\mu < 0$ (the incoming rays). The polarized spectrum is calculated by a two-stage process. The flowchart in Figure 6 shows the organization of these two stages.

RT Stage 1: A multi-level, PRD-capable code of Uitenbroek (2001), known as the RH-code, solves the statistical equilibrium equations and the unpolarized RT equations self-consistently. The RH-code yields the unpolarized intensity, the monochromatic opacities, and the collision rates at all the depth points in a model atmosphere. These quantities are then kept fixed and used for Stage 2. In the multilevel RH-code we use a Ca I model atom with 20 bound states, 17 line transitions and 19 continuum transitions. The main line is treated in PRD using the angle-averaged PRD functions of Hummer (1962). All other lines of the multiplet are treated with CRD. All the blend lines are treated in LTE.

The RT and the LSA approaches are implemented with several atmospheric models. Figure 2 shows the height dependence of the temperature structure and the thermalization parameter for the model atmospheres that we have tested. Among this set

of model atmospheres, FALX represents the coolest model, with the temperature minimum around 1000 km above the altitude zero corresponding to $\tau_{5000} = 1$. The results shown here have been obtained with the FALX model which seems the best choice for fitting the observations.

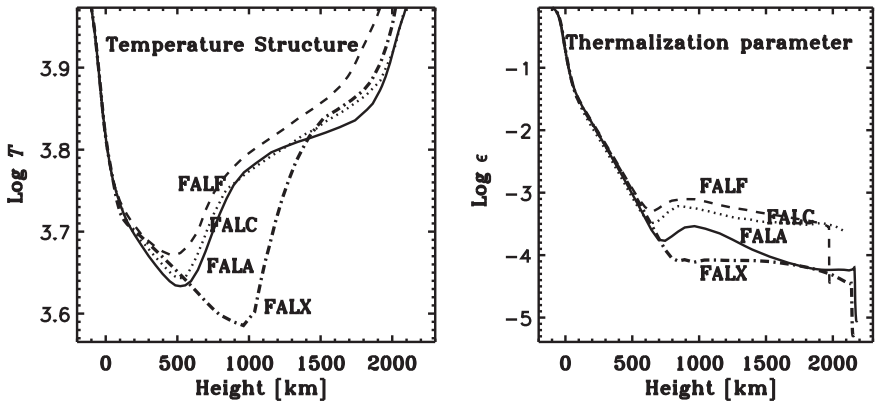

Figure 2. The height variation of the temperature and of the thermalization parameter, for different model atmospheres that we have tested in our attempts to fit the observed $(I, Q/I)$ profiles.

RT Stage 2: The Stokes vector $(I, Q)^T$ is computed by a perturbative type solution of the polarized transfer equation (see Fluri et al. 2003; Holzreuter et al. 2005).

3. The radiation anisotropy factor and its significance

A key factor which determines the shape of the emergent Q/I is the anisotropy of the radiation within the atmosphere, denoted here by k_G. It is given by

$$k_G(\lambda, \mu, \tau_\lambda) = \frac{3}{2\sqrt{2}}(1 - \mu^2) J_0^2(\lambda, \tau_\lambda)/I(\lambda, \mu, \tau_\lambda), \tag{6}$$

with

$$J_0^2(\lambda, \tau_\lambda) = \frac{1}{4\sqrt{2}} \int_{-1}^{+1} \mathrm{d}\mu' (3\mu'^2 - 1) I(\lambda, \mu', \tau_\lambda). \tag{7}$$

The factor k_G contains the dipole scattering phase matrix element responsible for producing the linear polarization and the anisotropic incident intensity $I(\lambda, \mu', \tau_\lambda)$ in Equation (7), which is necessary to generate the polarization. When the incident radiation field is isotropic, $k_G = 0$ and hence $Q/I = 0$.

The right panel in Figure 1 shows the height dependence of the anisotropy factor k_G at selected wavelengths. At each wavelength, k_G starts from zero inside the photosphere, shows a steep variation within the atmosphere, and saturates to a constant

maximum value when the radiation field becomes independent of height. In the saturation limit the anisotropy is the largest in the far wings and smaller at the line center. The maximum value occurs at heights where the source function gradient for a given wavelength is the largest (see Holzreuter et al. 2005, and references cited therein). The saturation value yields the value of k_G at the optical depth $\tau_\lambda = 0$.

4. The Last Scattering Approximation (LSA)

The concept of LSA implies that one first determines Stokes I, either through observations or with a numerical calculation in which the polarization is neglected. This is a reasonable approach in the case of the second solar spectrum because the polarization does not exceed a few percent. One then assumes that a single scattering of this intensity field suffices to properly evaluate the observed linear polarization. This LSA concept has been used in Stenflo (1982) to determine micro-turbulent magnetic fields on the Sun, in Stenflo (2005) for the solar continuum polarization, in Sampoorna et al. (2009) for the Hanle effect in the Ca I 4227 Å line, and in Belluzzi et al. (2007) for the Ba II D_1 and D_2 lines. In the above references, the Q/I is deduced from the observed Stokes I. In contrast, in Faurobert & Arnaud (2002), devoted to the linear polarization of molecular emission lines, Stokes I is deduced from the solution of an unpolarized RT equation.

In our use of LSA we first calculate Stokes $I(\lambda, \mu, \tau_\lambda)$ at all the depth points in a solar model atmosphere, ignoring the contribution of Stokes Q in the source terms. This is the Stage 1 of the RT approach. To obtain the polarization, we keep only the terms depending on Stokes I in the definition of the source term S_Q. Once S_Q has been obtained, the solution of a simple transfer equation yields Stokes Q. This method is closely related to the iterative method introduced in Frisch et al. (2009) to calculate the linear polarization. As done here, one neglects the polarization in the calculation of Stokes I, while retaining the polarization in the Q-component of the source term. One can thus establish an integral equation for S_Q. The first term in a Neumann series expansion (scattering expansion) of the solution is identical to the LSA approximation described here (see also Anusha et al. 2010).

The LSA approximation leads to

$$[S_{I,l}(\lambda, \tau_\lambda)]_{\rm LSA} = \epsilon B_\lambda(\tau_\lambda) + \frac{1-\epsilon}{\phi(\lambda, z)} \int_0^\infty {\rm d}\lambda' R^{(0)}(\lambda, \lambda', z) J(\lambda', \tau_{\lambda'}), \tag{8}$$

for the Stokes I line source function, where the mean intensity J is defined as

$$J(\lambda', \tau_{\lambda'}) = \int_{-1}^{+1} \frac{{\rm d}\mu'}{2} I(\lambda', \mu', \tau_{\lambda'}), \tag{9}$$

and to

$$[S_{Q,l}(\lambda, \mu, \tau_\lambda)]_{\rm LSA} = \frac{3}{2\sqrt{2}} \frac{1-\epsilon}{\phi(\lambda, z)} (1-\mu^2) \int_0^\infty {\rm d}\lambda' R^{(2)}(\lambda, \lambda', z) J^2_0(\lambda', \tau_{\lambda'}), \tag{10}$$

for the Stokes Q line source function, where $J^2_0(\lambda', \tau_{\lambda'})$ is defined in Equation (7). The angle-averaged PRD functions $R^{(0)}$ and $R^{(2)}$ can be found in Anusha et al. (2010). A

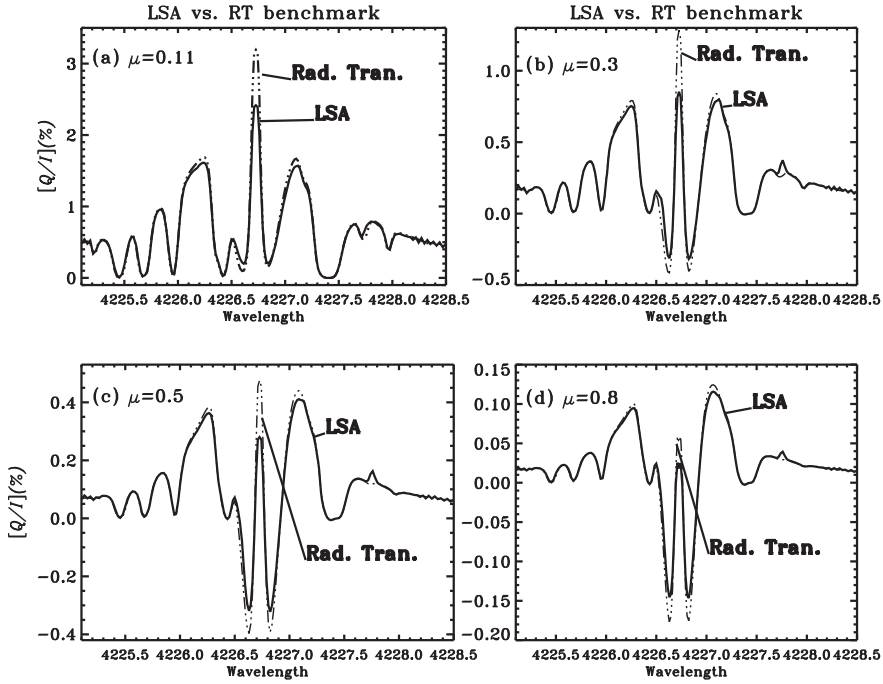

Figure 3. Comparison of Q/I computed by the LSA approach with the solution computed by the RT approach, for different values of the cosine of the heliocentric angle, μ. The model atmosphere used is FALX. The scaling parameter is $s = 1$ for all the panels.

similar approximation for the continuum source vector $\boldsymbol{S}_c$ is also made. Using the formal solution written in Equation (5) (neglecting the contribution from $\boldsymbol{I}_0$), we obtain for the emergent Q/I the approximate formula

$$\left[\frac{Q}{I}(\lambda,\mu)\right]_{\rm LSA} = s\,\frac{\int_0^{T_\lambda}\left(\mathrm{d}\tau'_\lambda/\mu\right)\exp\left(-\tau'_\lambda/\mu\right)\left[S_Q(\lambda,\mu,\tau'_\lambda)\right]_{\rm LSA}}{\int_0^{T_\lambda}\left(\mathrm{d}\tau'_\lambda/\mu\right)\exp\left(-\tau'_\lambda/\mu\right)\left[S_I(\lambda,\tau'_\lambda)\right]_{\rm LSA}}. \tag{11}$$

The quantity s is an ad-hoc scaling parameter. Its role is described below. Thus, with LSA, we can reduce the solution of a set of coupled integro-differential equations for $(I, Q)^T$ to the solution of a single scalar integro-differential equation followed by the evaluation of a simple formula for Q/I.

To validate the LSA approach, we have compared the ratio Q/I computed by the LSA and RT approaches for different values of μ. Figure 3 shows that the LSA results with $s = 1$ are in very good agreement with the RT curves. The tiny differences that exist between the two methods at line center are due to the neglect of scattering terms of order higher than one in the expression of S_Q.

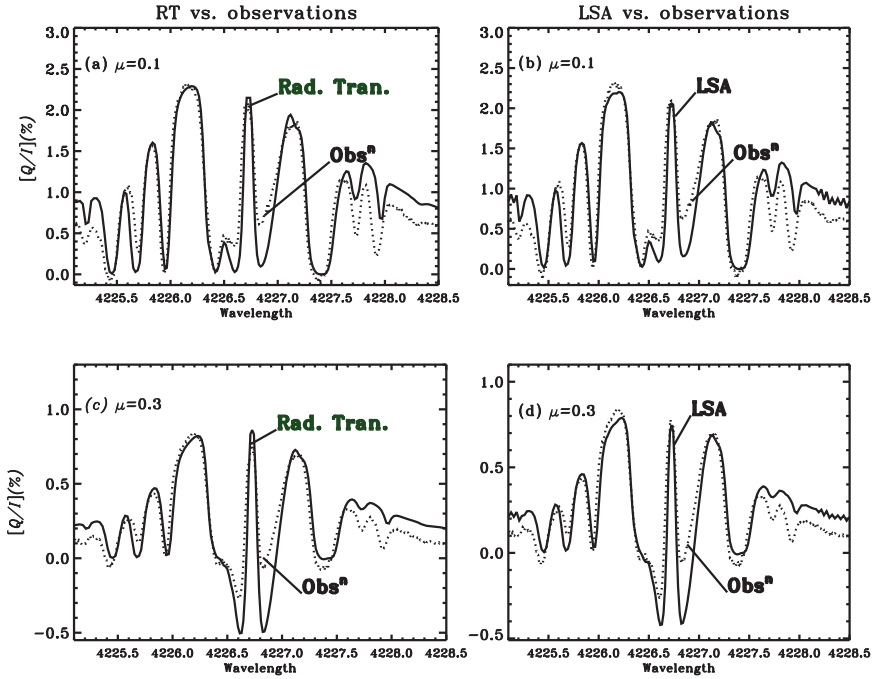

Figure 4. Comparison between the theoretical Q/I spectra computed with the RT and LSA approaches and the observations obtained in January 2010. The FALX model atmosphere has been used. The parameters required for the fits are: s=1.65, 1.8, 1.1 and 1.35, c = 1.5, B_{turb} = 30, 25, 20 and 15 G for panels (a)–(d) respectively.

5. The modeling of the observations with the LSA approach

Three free parameters are needed for the modeling of the observed Q/I profiles. They are: (i) c, (ii) s, and (iii) B_{turb}. Their roles are listed below and their values are given in the caption of Figure 4 where we compare the observed Q/I profiles with values given by the RT and the LSA approaches.

Enhancement parameter c : To fit the red and the blue peaks of Q/I, we introduce a parameter c, which multiplies the value of the elastic collision rate $\Gamma_{\rm E,vW}$ that is based on the van der Waal's theory (see e.g., Faurobert-Scholl 1992).

Scaling parameter s : The global scaling parameter s is introduced to fit the wings of the Q/I profiles calculated with either the RT approach or the LSA approach, to the shapes of the observed wings. For the choice of s one considers all the wavelengths starting from the near wings, red and blue peaks, and going all the way to the continuum (see e.g., Anusha et al. 2010). Ideally, s should be unity. Departures from unity indicate a modeling deficiency arising either from theory or from the observations. Possible causes for $s \neq 1$ are : (i) an inappropriate choice of model atmosphere, (ii) the use

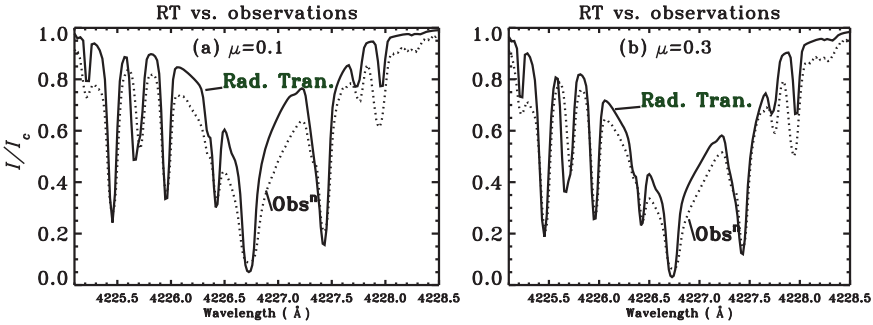

Figure 5. Comparison between theoretical Stokes I spectra, computed with the RT approach using the FALX model atmosphere, and observations obtained in January 2010.

of 1-D geometry to represent the solar atmosphere, (iii) the use of angle-averaged PRD functions, (iv) observational uncertainties in μ, caused by the limb curvature, the use of a long slit, as well as seeing, and (v) other unidentified sources of errors.

Micro-turbulent magnetic field strength B_{turb}: After determining c and s we still need a Hanle depolarization factor to fit the line core, which here comes in the form of a micro-turbulent magnetic field of strength B_{turb} (see e.g., Stenflo 1982). We assume that the micro-turbulent magnetic field vectors are isotropically distributed.

Figure 4 shows that the LSA and the RT approaches can provide a good fit to the observed Q/I if the free parameters are chosen properly. Note that the scaling parameter s remains between 1 and 2, that the enhancement parameter is 1.5, and that the micro-turbulent magnetic field strength is between 15 and 30 G. The value of B_{turb} is always smaller for the LSA than for the RT calculation because the LSA underestimates the core peak height (see Figure 3). The fact that s is not unity indicates a modeling deficiency clearly visible in Figure 5 where we compare the observed Stokes I profiles to the results of an RT calculation.

6. Conclusions

In this paper we have presented a theoretical framework to calculate the linear polarization of strong resonance lines, based on the last scattering approximation. Unlike a previous attempt (Sampoorna et al. 2009), we are now able to provide a detailed fit of the Q/I profile of the Ca I 4227 Å line by taking into account the depth-dependence of the radiation field anisotropy in the atmosphere. In particular, the LSA approach can provide a good fit to all the characteristic features of the Q/I spectrum: (i) core peak, (ii) minima about the line center, (iii) asymmetric PRD wing maxima, (iv) blend lines polarization, and (v) far wing polarization. Computationally, LSA is about 8 times faster than a full RT approach. Therefore the LSA appears to be an efficient approach

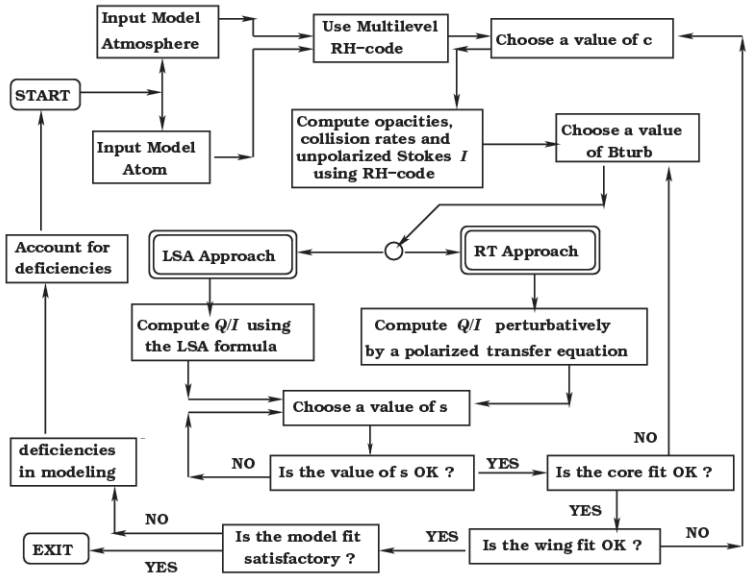

Figure 6. Flowchart showing the main computing steps in the RT and LSA approaches applied to the Ca I 4227 Å line.

to model the second (Q/I) solar spectrum, in particular when 3-D model atmospheres resulting from magneto-hydrodynamical numerical simulations are considered.

Acknowledgments. L. S. Anusha is grateful to the University of Hawaii Foundation for full financial support that enabled her to participate in the SPW6 workshop held at Maui, Hawaii.

References

Anusha, L. S., Nagendra, K. N., Stenflo, J. O., Bianda, M., Sampoorna, M., Frisch, H., Holzreuter, R., & Ramelli, R. 2010, ApJ, 718, 988
Belluzzi, L., Trujillo Bueno, J., & Landi Degl'Innocenti, E. 2007, ApJ, 666, 588
Bommier, V. 1997, A&A, 328, 726
Domke, H., & Hubeny, I. 1988, ApJ, 334, 527
Faurobert, M., & Arnaud, J. 2002, A&A, 382, L17
Faurobert-Scholl, M. 1992, A&A, 258, 521
— 1994, A&A, 285, 655
Fluri, D. M., Holzreuter, R., Klement, J., & Stenflo, J. O. 2003, in Astronomical Society of the Pacific Conference Series, edited by J. Trujillo-Bueno & J. Sanchez Almeida, vol. 307 of Astronomical Society of the Pacific Conference Series, 263
Frisch, H., Anusha, L. S., Sampoorna, M., & Nagendra, K. N. 2009, A&A, 501, 335
Holzreuter, R., Fluri, D. M., & Stenflo, J. O. 2005, A&A, 434, 713
Hummer, D. G. 1962, MNRAS, 125, 21
Sampoorna, M., Stenflo, J. O., Nagendra, K. N., Bianda, M., Ramelli, R., & Anusha, L. S. 2009, ApJ, 699, 1650

Sampoorna, M., Trujillo Bueno, J., & Landi Degl'Innocenti, E. 2010, ApJ, 722, in press
Stenflo, J. O. 1982, Sol. Phys., 80, 209
— 2005, A&A, 429, 713
Uitenbroek, H. 2001, ApJ, 557, 389